

Magnetic Multilayers

Eric Fullerton

Electrical and Computer Engineering
NanoEngineering
Center for Magnetic Recording Research
University of California San Diego



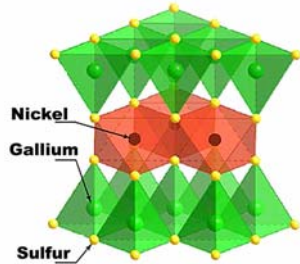
Magnetic Multilayers

Outline

- Introduction to magnetism
- X-ray techniques
 - Spectroscopy
 - Imaging
 - Scattering

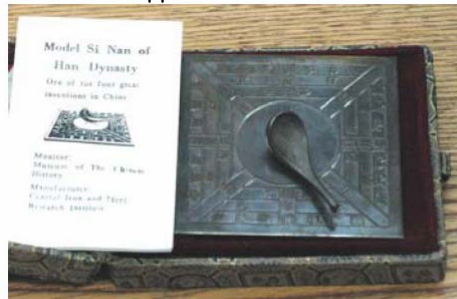
Magnetism

Atomic property



Collective response

applications



Model of compass used in China about 450 BC. The reference direction was south

3

Spin and orbital magnetic moment

$$\mu_B \equiv \frac{e\hbar}{2m} = 9.274 \cdot 10^{-24} \frac{J}{T} = 9.274 \cdot 10^{-24} \text{ emu}$$

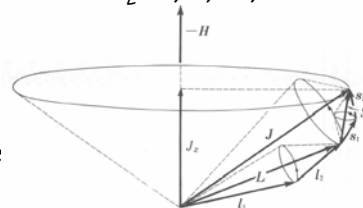
dipole moment created by electron on Bohr radius of the hydrogen atom, $a_B = 0.529 \text{ \AA}$

- **Spin magnetic dipole moment:** $\vec{\mu}_S = -\frac{e}{m} \vec{S}$
component of S is quantized, $S_z = m_S \hbar / 2\pi$ with $m_S = \pm 1/2$

- **Orbital magnetic moment** $\vec{\mu}_{orb} = -\frac{e}{2m} \vec{L}_{orb}$
component of L is quantized, $L_{orb,z} = m_L \hbar / 2\pi$ with $m_L = 0, \pm 1, \pm 2, \dots, \pm n-1$

- **Total moment** $\vec{J} = \vec{L} + \vec{S}$

- *Arrange electrons via Hund's rule*



Spin-Orbit Interaction

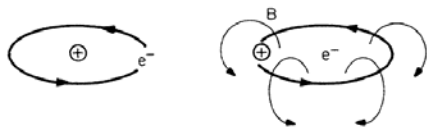


Figure 3.14 Diagram on left, depicts an electron orbiting about the nucleus. In the diagram on the right, from the electron's rest frame, the nucleus appears to be orbiting around the electron and hence producing a magnetic field in the sense indicated. The interaction of the electron spin with its orbitally induced magnetic field is the spin-orbit interaction.

Magnetic field experienced by electron due to motion relative to nucleus

$$\vec{B} = \frac{\mu_0}{4\pi} \cdot \frac{\vec{j} \times \vec{r}}{r^3} = -\frac{Ze\mu_0}{4\pi} \left(\frac{\vec{v} \times \vec{r}}{r^3} \right)$$

Spin-orbit interaction

- only for orbitals with $L \neq 0$
- atomic number Z implicit in $V \Rightarrow$ stronger for heavier atoms

$$\Delta E_{so} = \frac{1}{2m^2c^2} \cdot \frac{1}{r^3} \cdot \frac{\partial V}{\partial r} \vec{L} \cdot \vec{S}$$

5

3d transition metals vs. 4-f rare-earth elements

magnetism carried by
 - 3d electrons: outer shell
 - 4f electrons: inner shell
 results in different properties

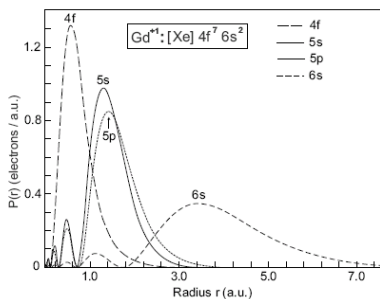
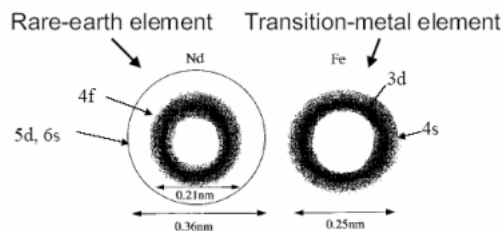
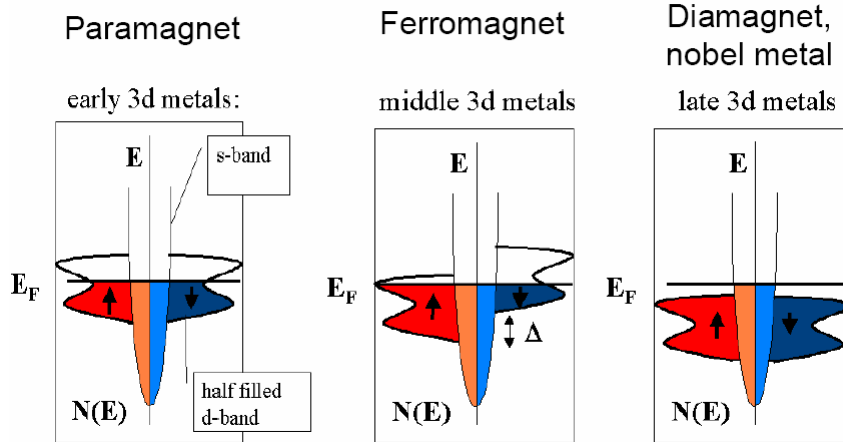


Fig. 7.4. Radial charge density for the Gd^{+3} ion ($4f^7 6s^2$) calculated by Freeman and Watson [204] for the $4f$, $5s$, $5p$ and $6s$ orbitals. The figure shows that the $4f$ orbitals are actually located well inside the outer shells which screen them from the extra-atomic environment

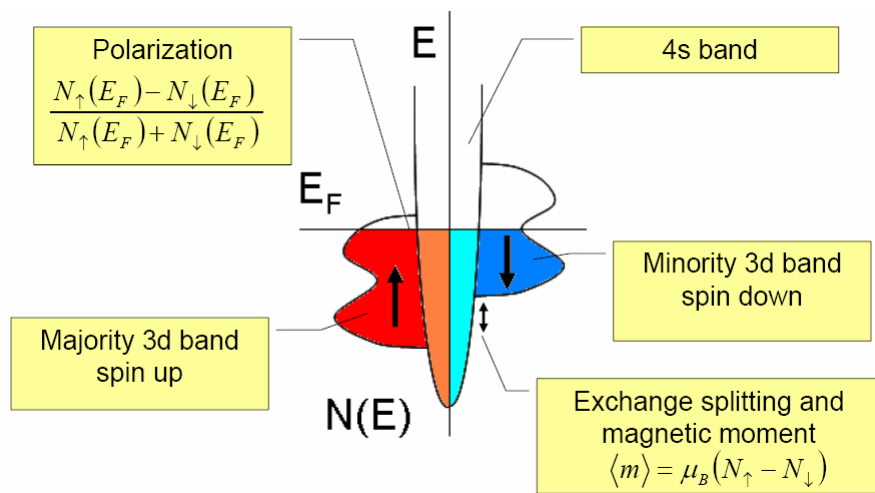
6

Band magnetism



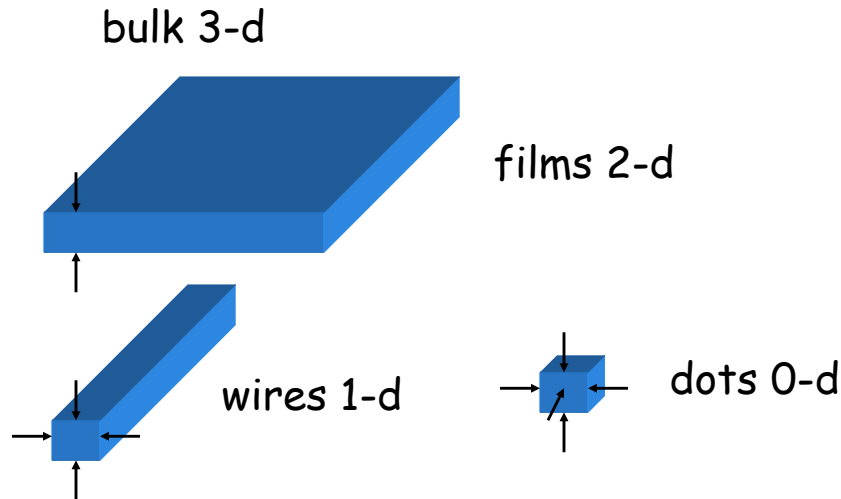
7

Band magnetism



8

Nano-structures



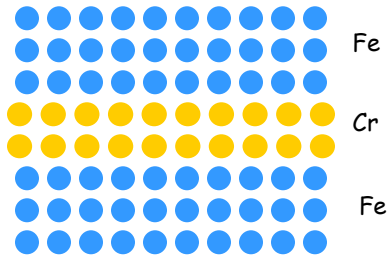
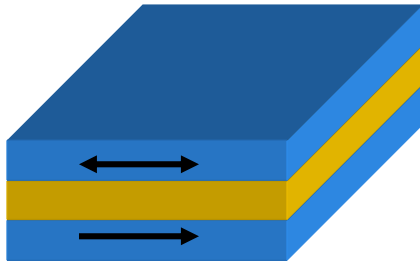
Nanomagnetism: length scales?

Characteristic length scales (metals)

- exchange and λ_F : <1 nm
 - (semiconductors $\lambda_F \sim 100$ nm)
- e^- mean free path: ~ 10 nm
- spin diffusion length: 1 - 1000 nm
- RKKY: 0.4 - 5 nm
- exchange length: 5 nm
- Dipolar: all length scales

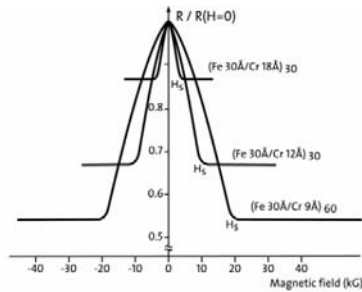
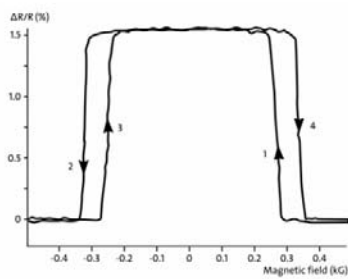
Nano-structures

Indirect effects



11

Giant magnetoresistance (GMR)



VOLUME 61, NUMBER 21

PHYSICAL REVIEW LETTERS

21 NOVEMBER 1988

Giant Magnetoresistance of (001)Fe/(001)Cr Magnetic Superlattices

M. N. Baibich,^{1,2} J. M. Broto, A. Fert, F. Nguyen Van Dau, and F. Petroff

PHYSICAL REVIEW B

VOLUME 39, NUMBER 7

1 MARCH 1989

Enhanced magnetoresistance in layered magnetic structures with antiferromagnetic interlayer exchange

G. Binasch, P. Grünberg, F. Saurenbach, and W. Zinn

12

Nobel Prize in Physics 2007



KUNGL.
VETENSKAPSAKADEMIEN
THE ROYAL SWEDISH ACADEMY OF SCIENCES



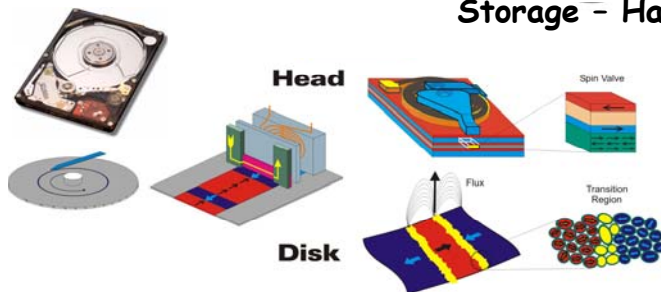
Peter Grunberg

Albert Fert

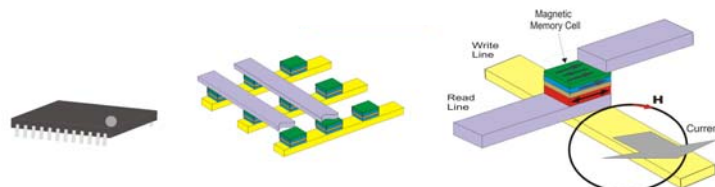
13

Magnetic Nanotechnologies

Storage - Hard Disk Drive

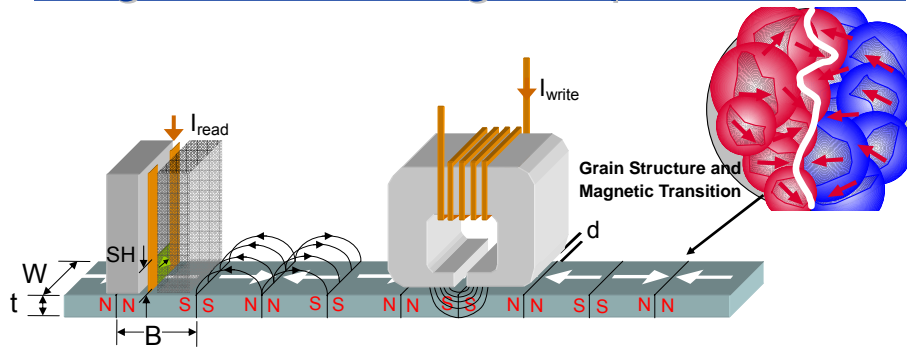


Memory - MRAM, FeRAM



14

Magnetic recording components



$B = 30 \text{ nm}$ ($\sigma < 3 \text{ nm}$),
 $W = 210 \text{ nm}$, $t = 14 \text{ nm}$
Data rate: GHz

15

Magnetic nanostructures

- Important new physics (e.g. Nobel Prize)
- Important technologies
 - Sensors (bio-magnetism, auto, ...)
 - IT (storage, memory, processing)
 - Energy efficiency

16

Magnetic nanostructures

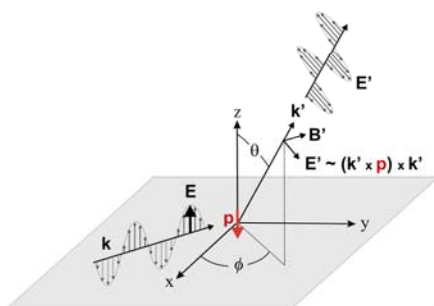
- Want to link structure and magnetism
 - atomic depth resolution
 - <10 nm lateral resolution
 - < 1 ns temporal resolution
- neutrons
- electrons
- scanning probe
- x-rays

} have a spin

17

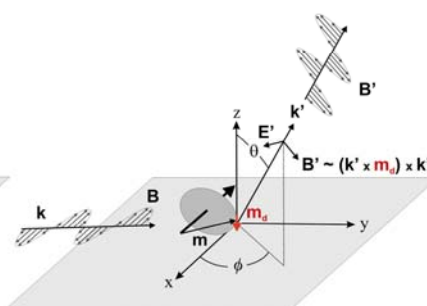
Non-resonant scattering

Electric Dipole Scattering



Relative Intensity: **1**

Magnetic Dipole Scattering



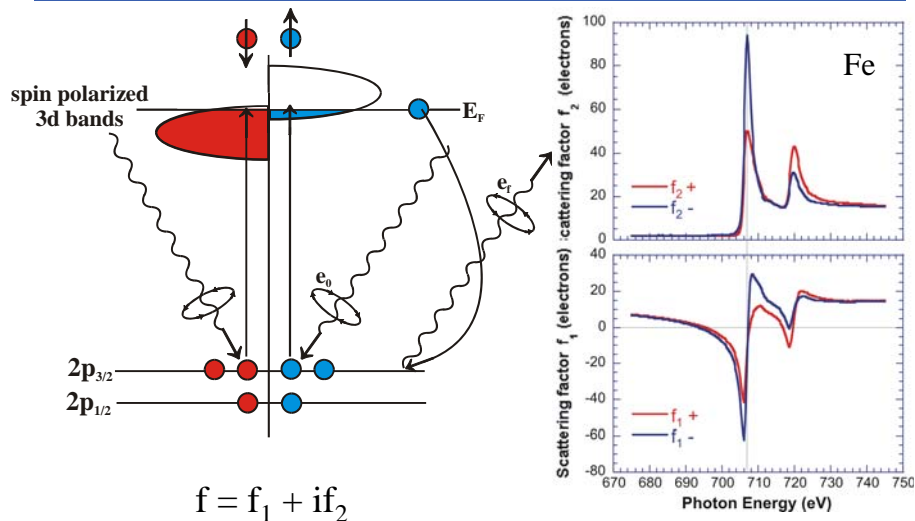
Relative Intensity: $(h\nu / mc^2)^2$

$h\nu \sim 10 \text{ keV}, mc^2 = 500 \text{ keV}$

X-rays typically are not very sensitive to magnetism

18

Core level resonances

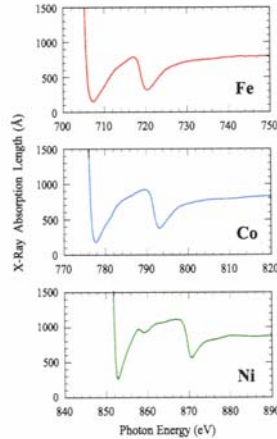
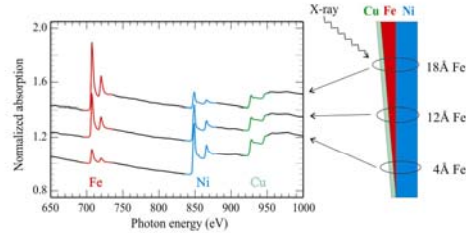


Soft x-ray techniques

- 3d-transition metal L-edges $2p \rightarrow 3d$ transitions (550-900 eV)
- rare-earth M-edges $3d \rightarrow 4f$ transitions (800-1600 eV)
 $\lambda = 1 - 2$ nm
- tuning **energy** gives **element** specificity
- tuning **polarization** gives **magnetic** specificity
- Various spectroscopy, imaging, optical and scattering techniques with nm resolution
 For reviews see
 - Kortright *et al.*, J. Magn. Magn. Mater. **207**, 7 (1999).
 - Srajer *et al.*, J. Magn. Magn. Mater. **307**, 1-36 (2006).

Elemental and chemical sensitivity

X-rays can pick materials apart: layer-by-layer



X-rays offer chemical sensitivity

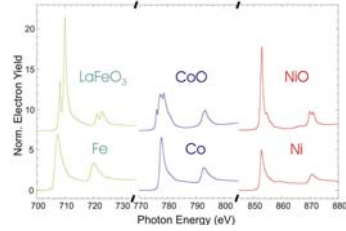


Fig. 8. X-ray absorption length ($1/e$ attenuation) for Fe, Co and Ni in the L edge region.³⁷ The absorption lengths in the pre-edge regions (not shown) are about 600 nm.

Stohr *et al.*, Surf. Rev. Lett. **5**, 1297 ('98).

Spectroscopy

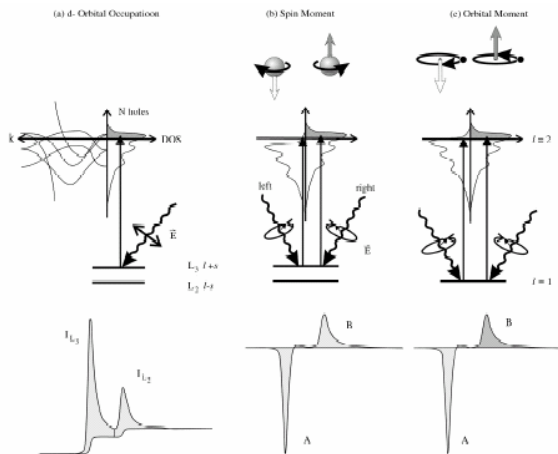


Fig. 1. (a) Electronic transitions in conventional L-edge X-ray absorption, (b) and (c) X-ray magnetic circular dichroism, illustrated in a one-electron model. The transitions occur from the spin-orbit split $2p$ core shell to empty conduction band states above the Fermi level. In conventional X-ray absorption the transition intensity measured as the white line intensity $I_{L_3} + I_{L_2}$ is proportional to the number of d holes, N . By use of circularly polarized X-rays the spin moment (b), and orbital moment (c), can be determined from the dichroic difference intensities A and B , as explained in the text.

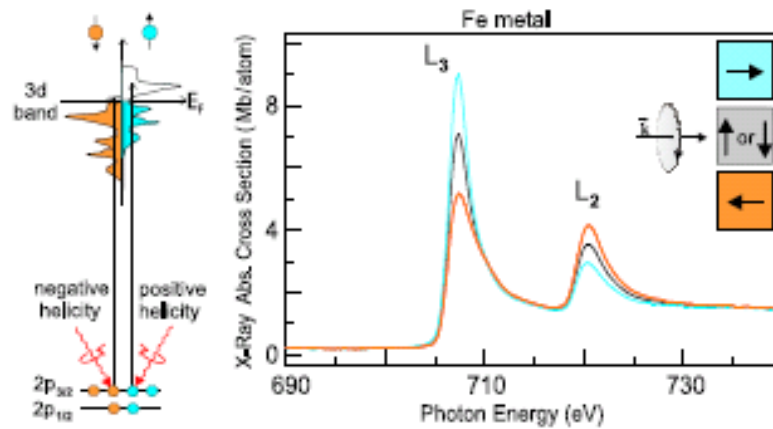
J. Stohr, JMMM 200, 470 (97).

Measures average Properties

MCD (magnetic circular dichroism)

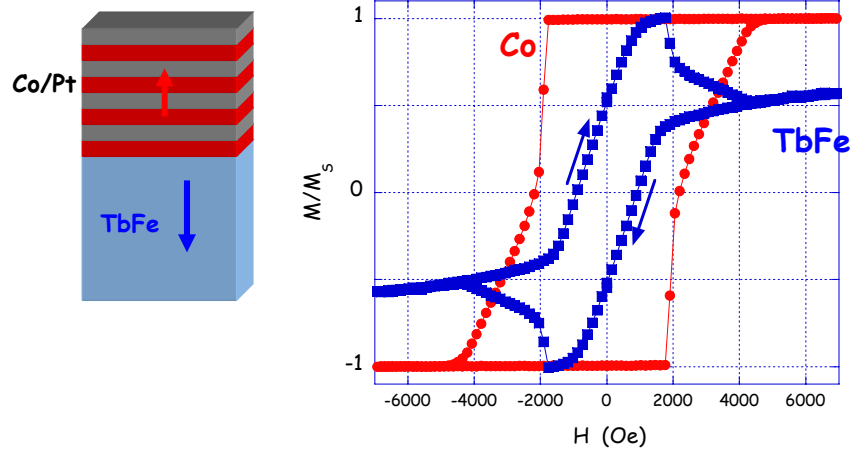
- e.g.
- d-band filling
- Moment
 - spin
 - orbital
- hysteresis loops

Element specific magnetometry



23

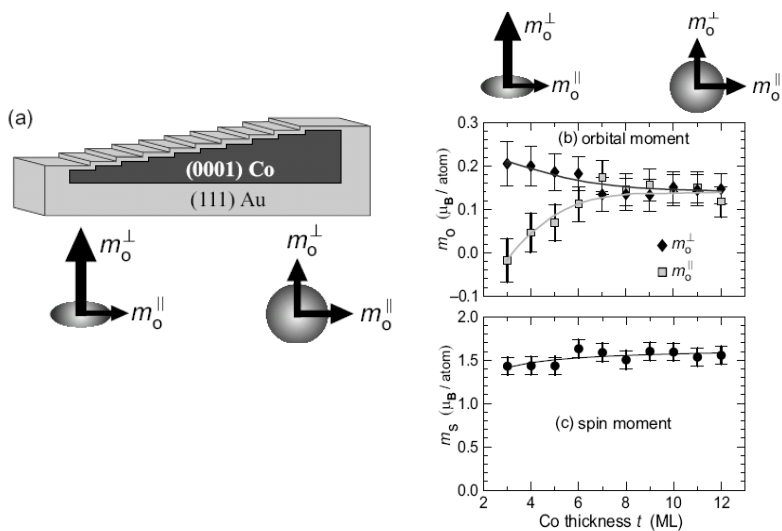
Elemental and chemical sensitivity



S. Mangin et al., Phys. Rev. B **78**, 024424 (2008)

24

Spin and orbital moments

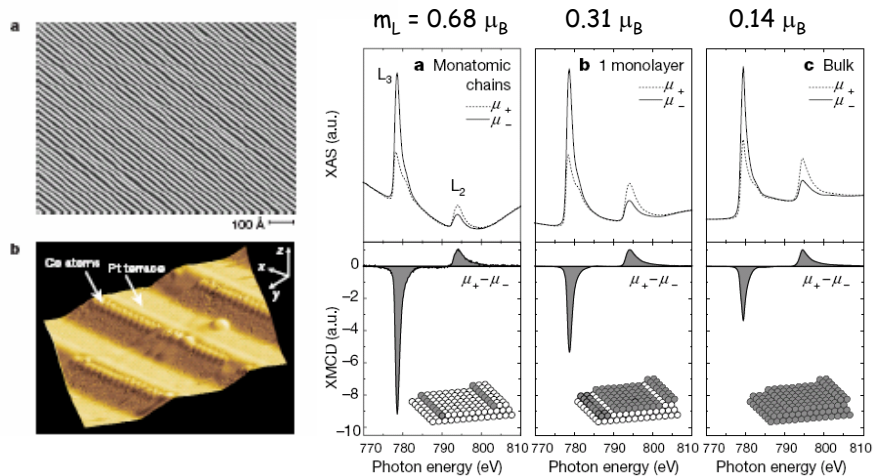


25

Spin and orbital moments

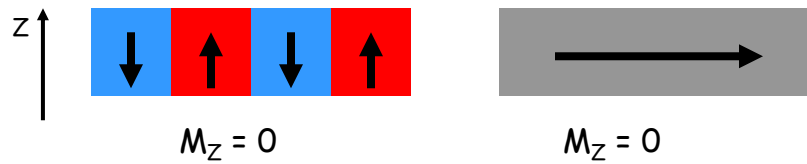
Ferromagnetism in one-dimensional monatomic metal chains

Gambardella, *et al.*, Nature **416**, 301 (2002)



Spatial sensitivity

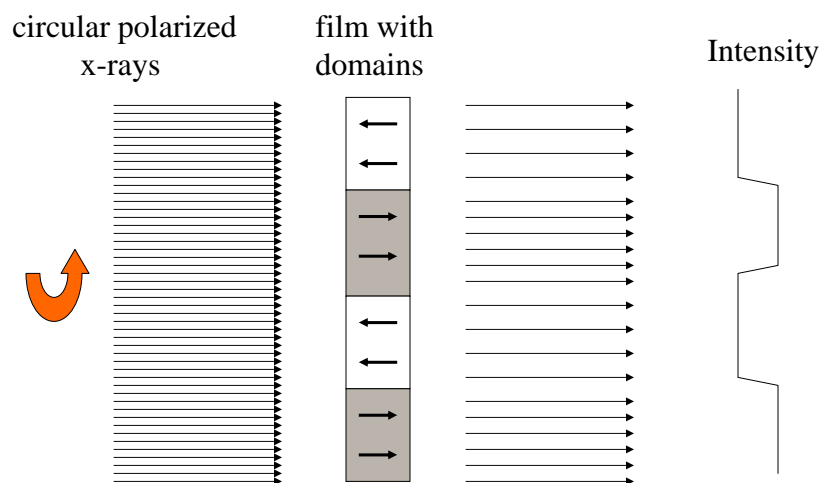
Spectroscopy gives you an average response of the atoms in systems



Spatial variations require either imaging or scattering

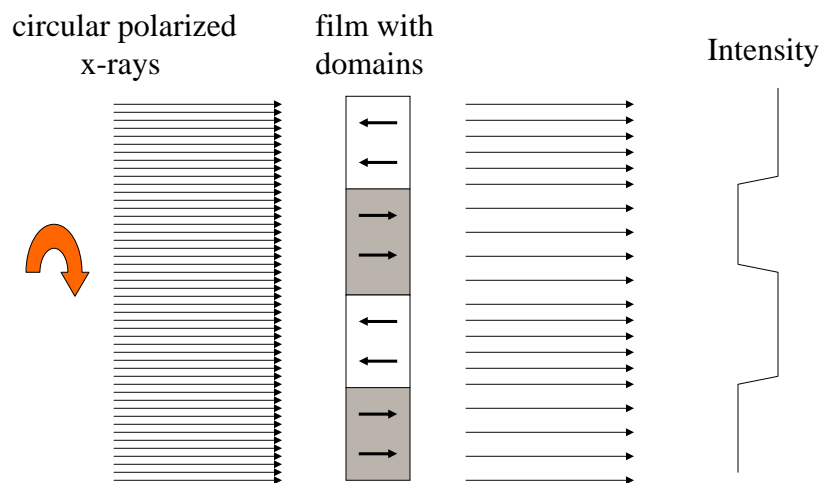
27

Magnetic Microscopy



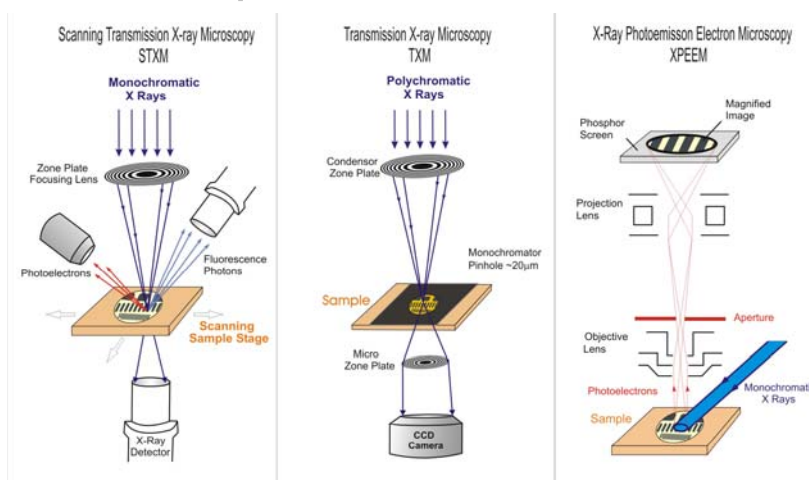
28

Magnetic Microscopy



Magnetic contrast is the difference of the left and right circular polarization 29

Microscopes at the ALS

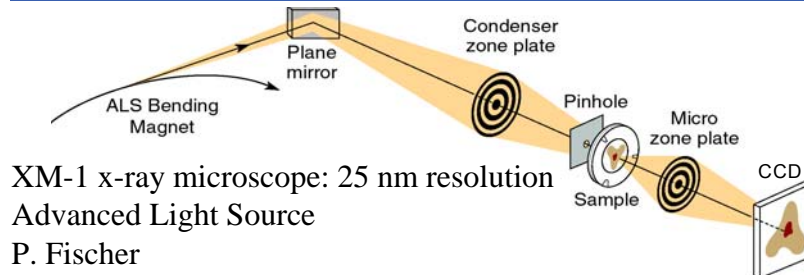


Present resolution in the 20 - 40 nm range

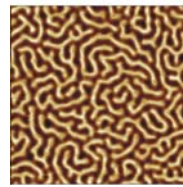
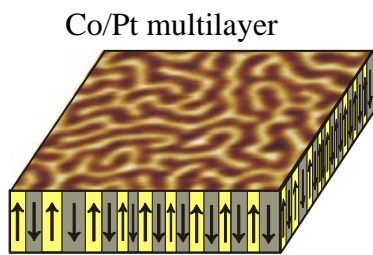
<http://www-als.lbl.gov/als/microscopes/index.html>

30

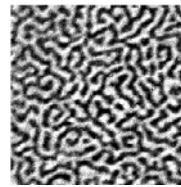
Domains in Co/Pt ML's



XM-1 x-ray microscope: 25 nm resolution
Advanced Light Source
P. Fischer



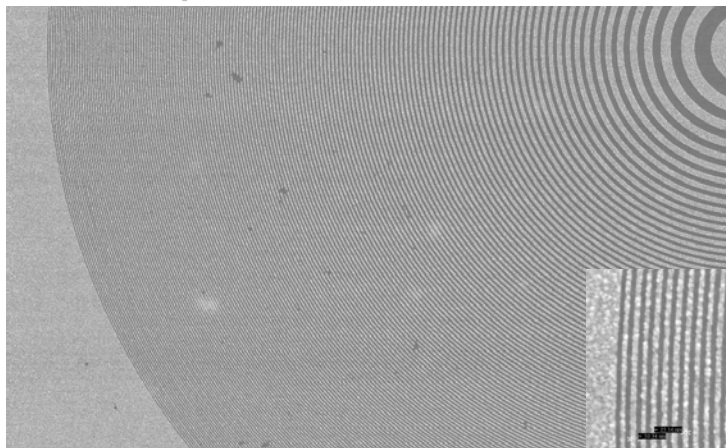
MFM
stray fields



XM-1
magnetization

31

Zone plates



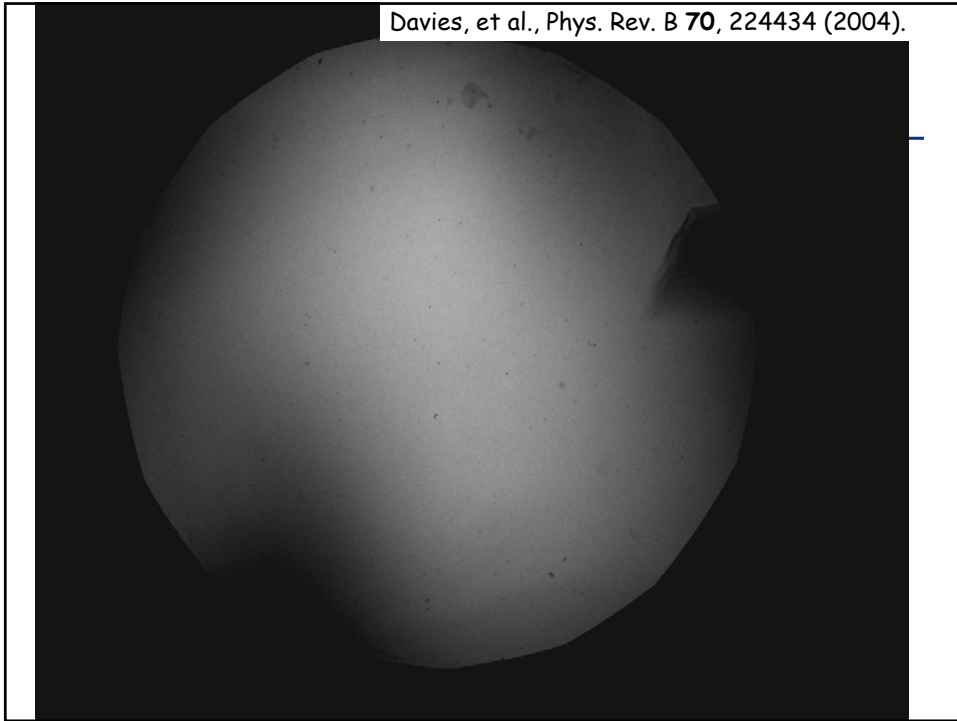
- $\Delta r = 25 \text{ nm}$
- $D = 63 \mu\text{m}$
- $N = 618 \text{ zones}$

E. Anderson, B. Harteneck, D. Olynick, E. Veklerov / CXRO

- **Zone plate manufacturability limits spatial resolution**
- **State of the art resolution is 20-30nm**

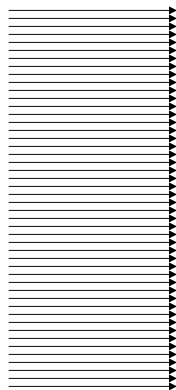
32

Davies, et al., Phys. Rev. B 70, 224434 (2004).

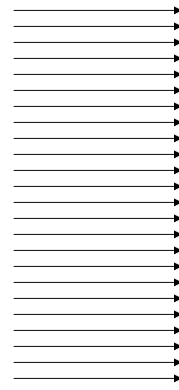


Vector magnetic microscopy

circular polarized
x-rays



film with
domains

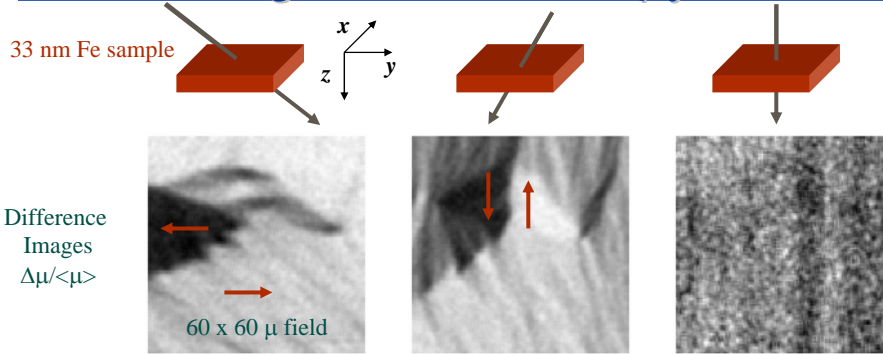


Intensity



34

Vector magnetic microscopy



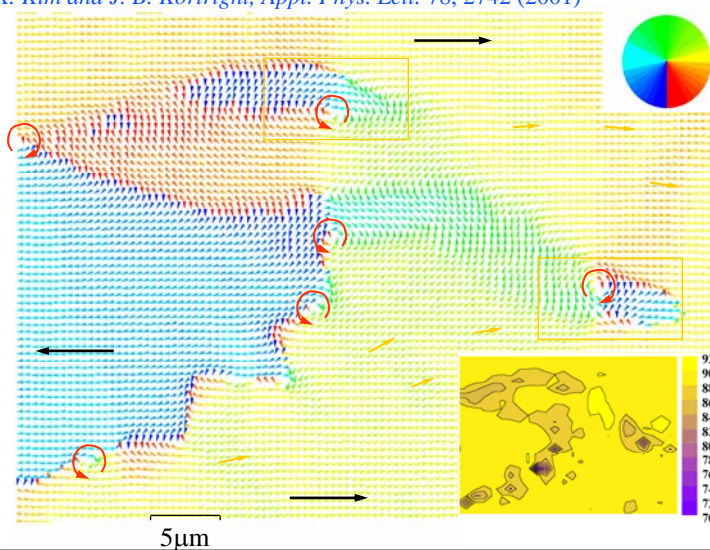
$$\begin{pmatrix} M_x \\ M_y \\ M_z \end{pmatrix} = \begin{pmatrix} k_{1x} & k_{1y} & k_{1z} \\ k_{2x} & k_{2y} & k_{2z} \\ k_{3x} & k_{3y} & k_{3z} \end{pmatrix}^{-1} \begin{pmatrix} \Delta\mu_1 \\ \Delta\mu_2 \\ \Delta\mu_3 \end{pmatrix}$$

$$|\mathbf{M}| = (M_x^2 + M_y^2 + M_z^2)^{1/2}$$

S. K. Kim and J. B. Kortright, *Appl. Phys. Lett.* 78, 2742 (2001) 35

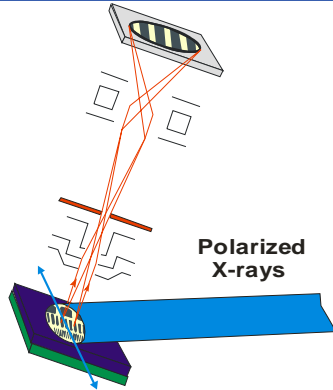
Vector magnetic microscopy

S. K. Kim and J. B. Kortright, *Appl. Phys. Lett.* 78, 2742 (2001)

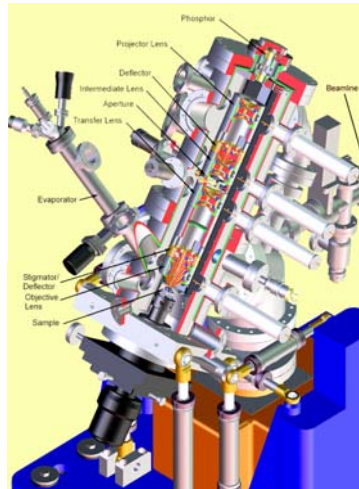


36

Domains in LaFeO_3/Co films



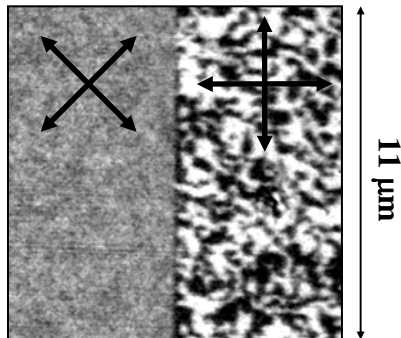
- Full Field Imaging
- Electrostatic (30 kV)
- 20 - 50 nm Resolution
- Linear and circular polarization



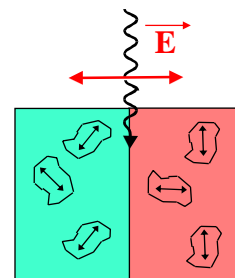
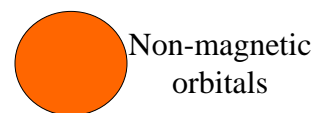
37

Domains in LaFeO_3 films

LaFeO_3 is an antiferromagnetic material

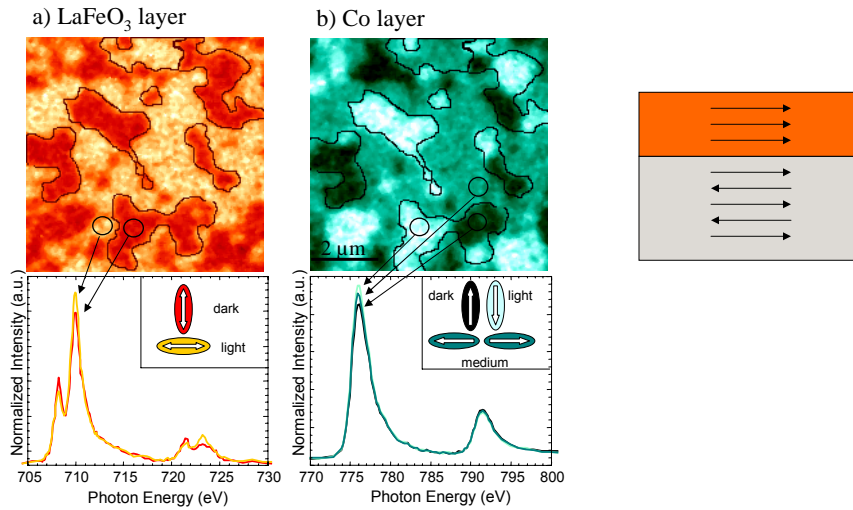


Scholl *et al.*, Science **287**, 1014 (2000)



38

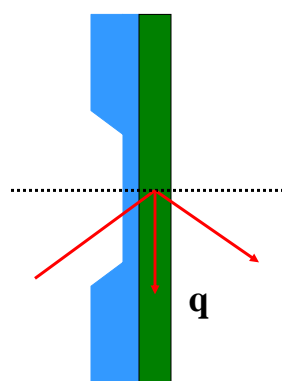
Domains in LaFeO₃/Co films



Nolting *et al.*, Nature **405**, 767 (2000)

39

Small-angle scattering (SAS)



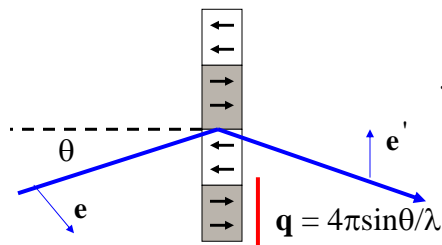
scattering arises from in-plane inhomogeneities (2-300 nm)

- Microstructure
- Grains
- Chemical segregation
- lithography
- Magnetic disorder (*e.g.* domains)

Kortright *et al.*, Phys. Rev. B **64**, 092401 (2001)

40

Magnetic domain scattering



$$f_n = \mathbf{e} \cdot \mathbf{e} F_n^{(0)} - i(\mathbf{e}' \times \mathbf{e}) \cdot \mathbf{M}_n F_n^{(1)}$$

charge magnetic -XMCD

$$I = \left| \sum_n f_n \exp(i\mathbf{q} \cdot \mathbf{r}_n) \right|^2$$

magnetic scattering

$$f_n \sim \mathbf{M}_n$$

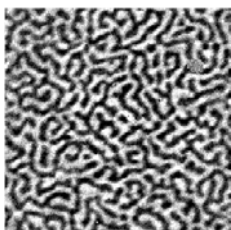
Scattering \sim |Fourier Transform|² of the domains

41

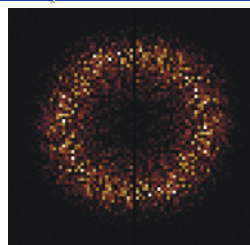
Real vs. reciprocal space

Domains in a Co/Pt ML

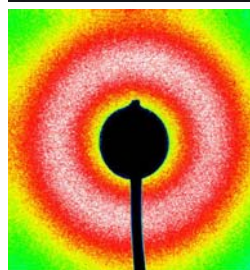
5 x 5 μm^2



XM-1
Imaging x-ray microscope



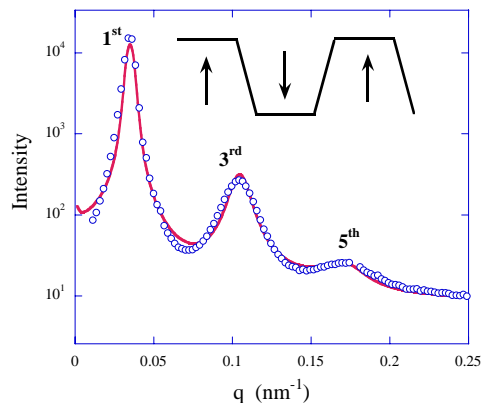
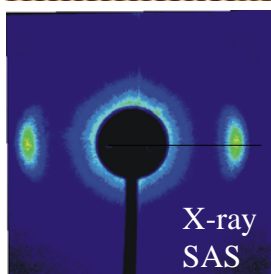
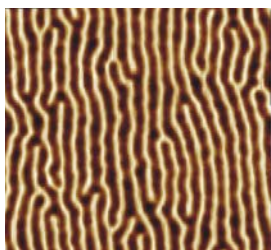
FT



Magnetic SAS
 $\sim |\text{FT}|^2$

42

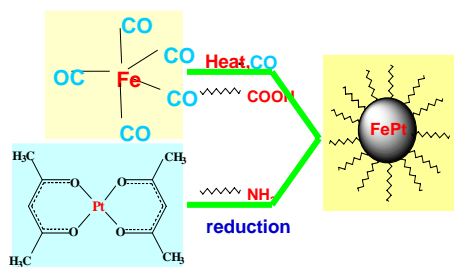
Aligned domains



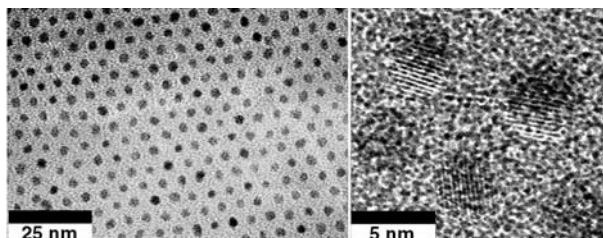
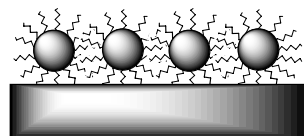
Hellwig *et al.*, Physica B **336**, 136 (2003).

43

Example 2: nanoparticle arrays



particles are coated
with Oleic acid and
oleyl amine

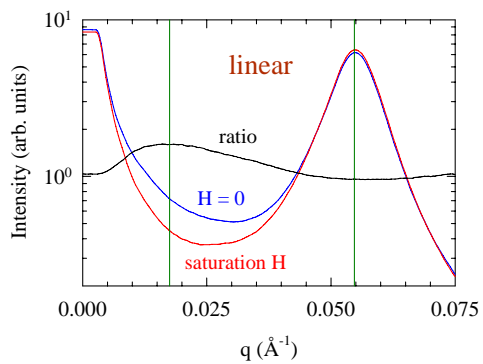
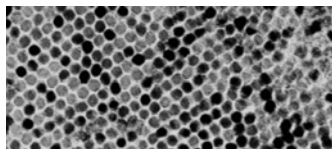


Tune: particle size
and separation

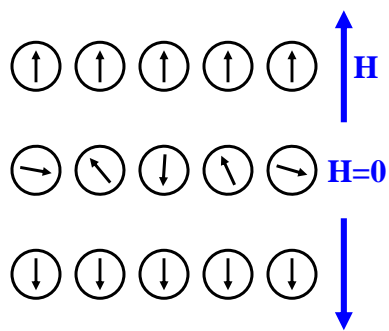
S. Sun
IBM

44

9-nm Co particle arrays



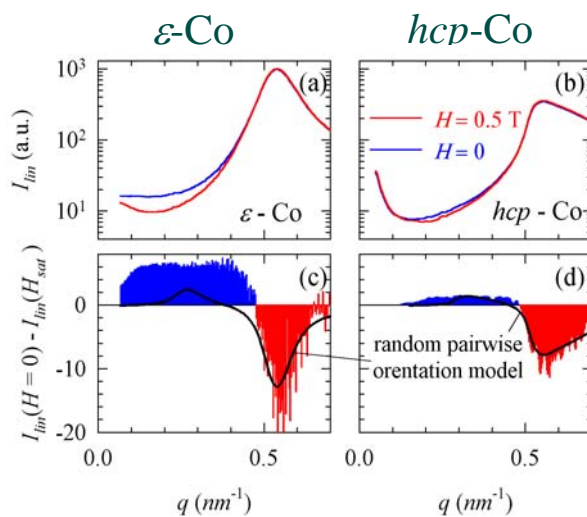
Superparamagnetic at room temperature



Magnetic structure at H=0?

45

Magnetic scattering



Kortright et al., Phys. Rev. B **71** 012402 (2005)

46

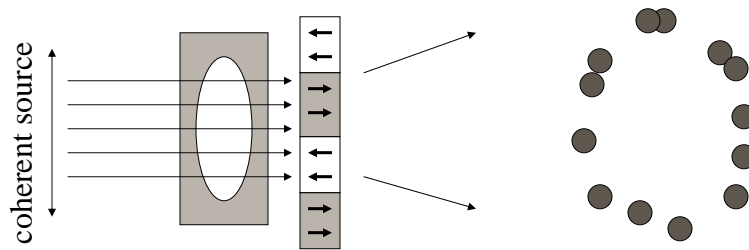
X-rays & Magnetism

Imaging: specific patterns
w/ relatively poor resolution

Scattering: statistical
information w/ good
resolution

The image shows the cover of the journal 'SRN Synchrotron Radiation News', November/December 2004, Vol. 17, No. 6. The cover features a grid of 12 images: four circular diffraction patterns in the top-left, four rectangular images in the top-right, and four rectangular images in the bottom-right. The text 'Focus on Magnetism' is centered on the cover. The Taylor & Francis logo is in the top right corner.

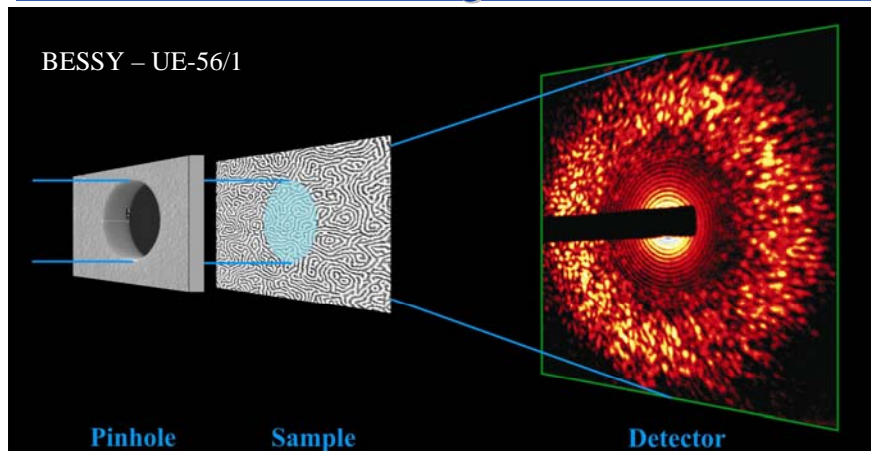
Coherent scattering (speckle)



Undulator ALS
Wavelength 16 Å
T correlation length ~ 40 μm (19,000 λ)
L correlation length > 13,000 Å (800 λ)
Coherent flux ~ 10¹² photons/second

Pattern encodes the spatial
distribution of the domain.

Coherent scattering



S. Eisebitt et al., Phys. Rev. B **68**, 104419 (2003).

49

Speckle

Metrology

configurational changes (H, T etc.)

Pierce et al., Phys. Rev. Lett., **90**, 175502 (2003).

Dynamics

configurational changes (time)

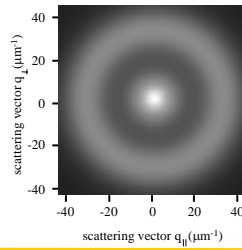
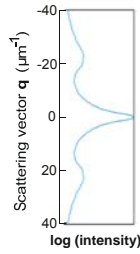
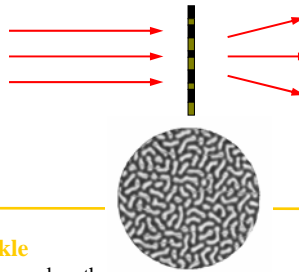
Shpyrko et al., Nature **447**, 68-71 (2007)

Data Inversion to real space

50

Incoherent vs. coherent scattering

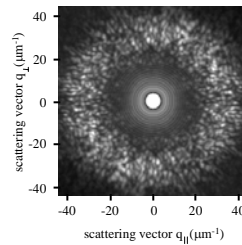
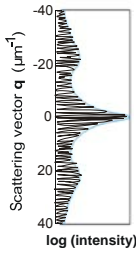
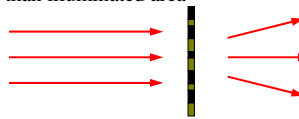
Coherence length larger than domains,
but smaller than illuminated area



information
about
domain
statistics

Speckle

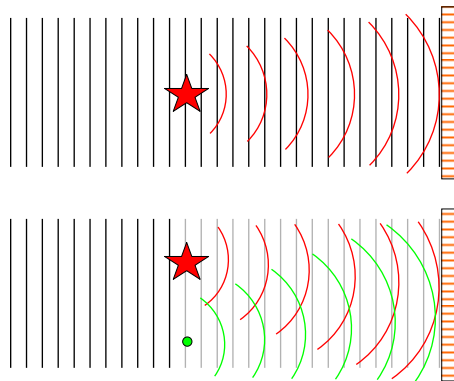
Coherence length
larger than illuminated area



true
information
about
domain
structure

51

Fourier Transform Holography

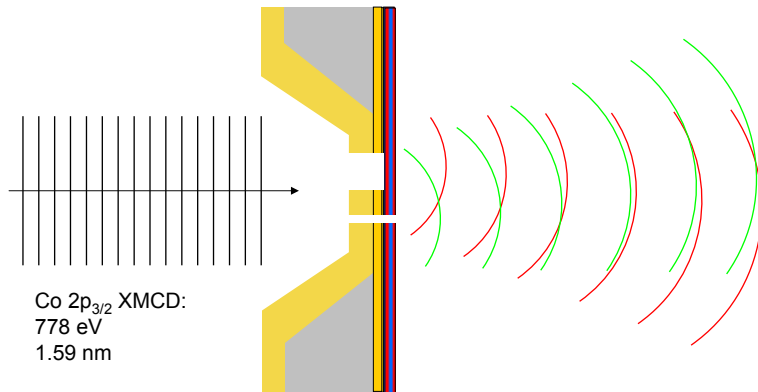


J.T. Winthrop, C.R. Worrington, Phys. Lett. 15, 124 (1965)

G.W. Stroke, *Lessless Fourier-transform method for optical holography*, APL 6, 201-203 (1965)

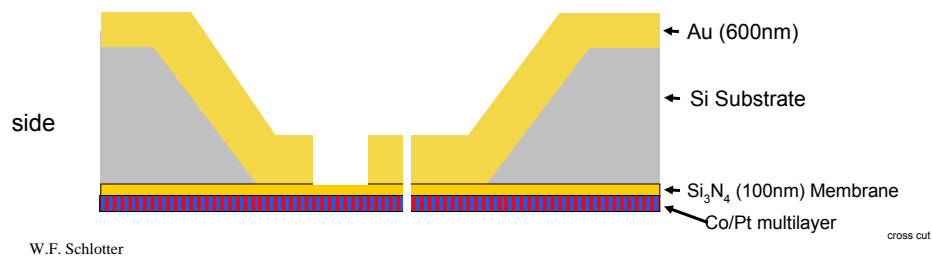
52

Fourier Transform Holography



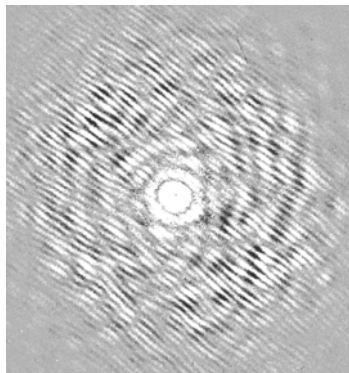
53

Fourier Transform Holography

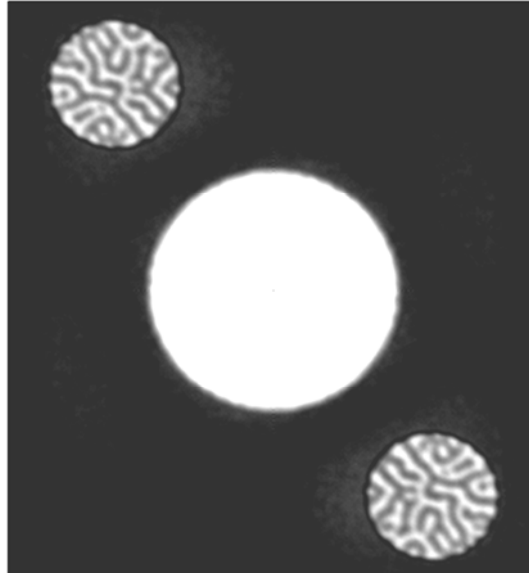


54

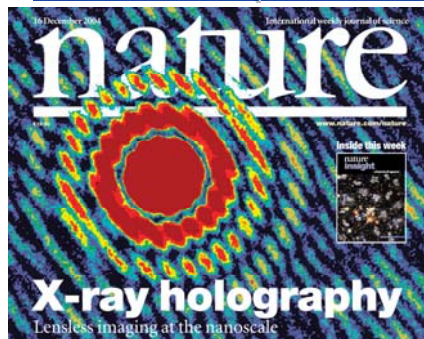
... the real space image



I^+ - I^-
**charge-magnetic
interference**



Microscope on a chip



16 December 2004

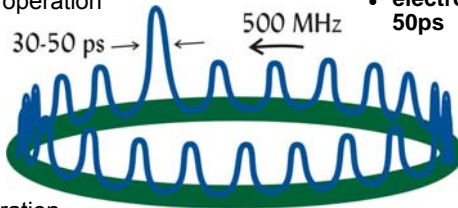
S. Eisebitt, J. Lüning, W. F. Schlotter, M. Lörger, O. Hellwig, W. Eberhardt, J. Stöhr, *Nature* **432**, 885 (2004)

‘Microscope on a chip’
• stable image area
• high fields/low temperature

Apply to a range of materials
science problems

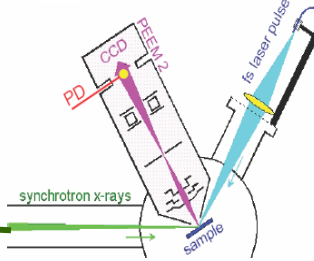
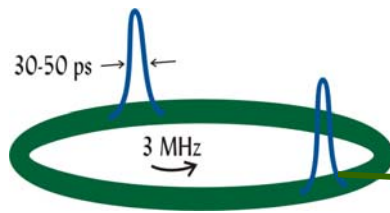
Time-resolved measurements

multi-bunch operation



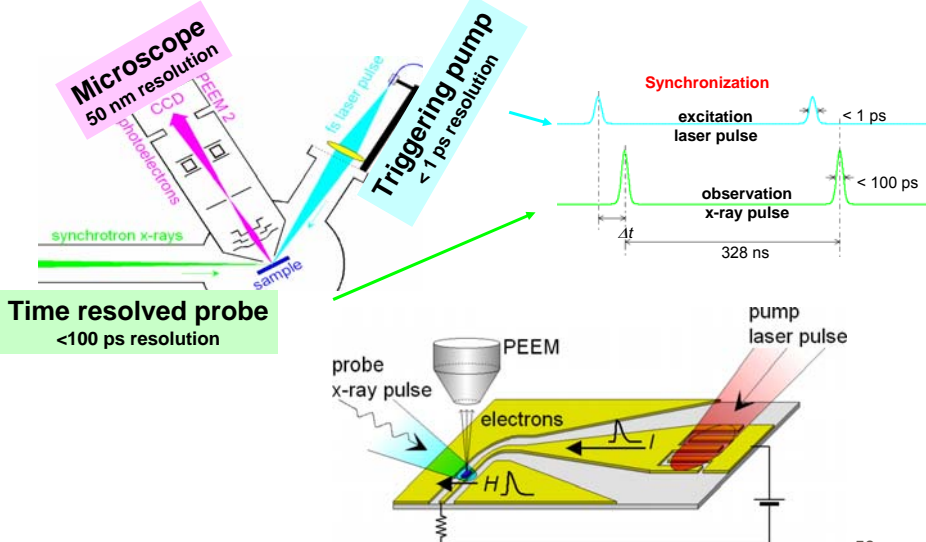
• electron-bunches typically 30-50ps

2-bunch operation



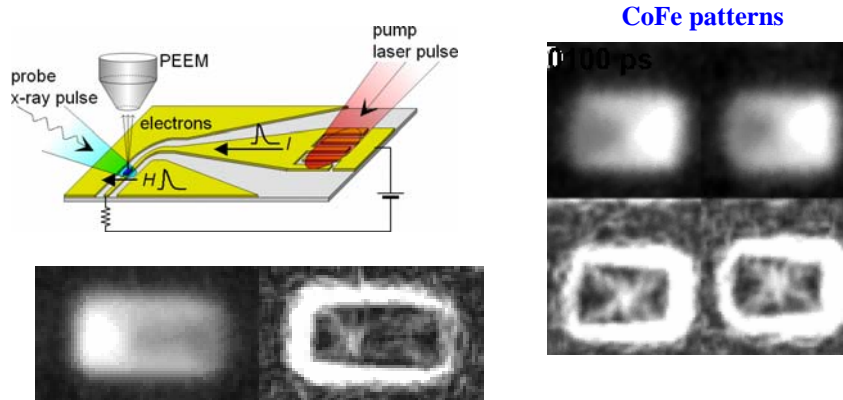
57

Synchrotron x-ray techniques



58

Synchrotron x-ray techniques



S.-B. Choe, et al., Science **304**, 430 (2004)

Measures only deterministic processes

59

Summary: X-rays and magnet nanostructures

- Resonant soft x-ray techniques provides nm-resolved magnetic and chemical information of heterogeneous films
- Spectroscopy: spin/orbital moments, DOS, etc.
- Imaging: real space (20 nm resolution)
- Scattering: reciprocal space (< 10 nm res.)
- Coherent scattering provides new opportunities.
- Pump-probe techniques give time resolved measurements

60